

Nanoscale

Accepted Manuscript



This is an *Accepted Manuscript*, which has been through the Royal Society of Chemistry peer review process and has been accepted for publication.

Accepted Manuscripts are published online shortly after acceptance, before technical editing, formatting and proof reading. Using this free service, authors can make their results available to the community, in citable form, before we publish the edited article. We will replace this *Accepted Manuscript* with the edited and formatted *Advance Article* as soon as it is available.

You can find more information about *Accepted Manuscripts* in the [Information for Authors](#).

Please note that technical editing may introduce minor changes to the text and/or graphics, which may alter content. The journal's standard [Terms & Conditions](#) and the [Ethical guidelines](#) still apply. In no event shall the Royal Society of Chemistry be held responsible for any errors or omissions in this *Accepted Manuscript* or any consequences arising from the use of any information it contains.

COMMUNICATION

Transport Behaviors of Photo-Carriers across Aligned Carbon Nanotubes and Silicon Interface

Cite this: DOI: 10.1039/x0xx00000x

Ru Li,^{a,b} Hongfang Li,^b Jingyun Zou,^b Xiaohua Zhang,^b and Qingwen Li^{b,*}

Received 00th January 2012,

Accepted 00th January 2012

DOI: 10.1039/x0xx00000x

www.rsc.org/

Transport of photo-carriers across the aligned carbon nanotubes and silicon (CNTs/Si) interface determines cell performance. It's revealed that S-shaped current-voltage characters are generated due to the mismatch between the generation and transportation of photo-carriers, which can be eliminated by tuning light intensity and CNT coverage on Si surface, with power conversion efficiency enhanced up to 121 %.

The transportation of photo-carriers across the carbon nanotubes and silicon (CNTs/Si) interface plays a critical role in CNTs/Si based solar cells¹⁻⁸ and photodetectors^{9, 10}. To date, the p-n junction,² heterojunction,⁷ schottky junction (MS)⁶ and MIS junction⁸ models have been extensively developed to understand the transport behaviors of photo-carriers across the interface. Physically, the diode model can be used to interpret the transport characters of CNTs/Si interface in dark condition. As illuminated, the photo-carriers are generated in Si, dissociated with the help of built-in electric field, and then transport across the CNTs/Si interface. Normally, the current-voltage (*I-V*) character of such an illuminated interface is a shift of the *I-V* character in dark condition. However, the illuminated CNTs/Si interface usually exhibits an S-shaped *I-V* character with degraded power conversion efficiency (Fig.1b), which has been widely observed in recent related publications.^{1, 3, 11, 12} The S-shaped *I-V* characters have been intensively studied in organic solar cells,^{13, 14} where the interface dipole, reduced surface recombination are considered to be the main sources. For the CNTs/Si based solar cells, Wadhwa et al.¹¹ used ionic liquid gate to reversibly generate and eliminate the S-shaped *I-V* characters, and claimed that the liquid gate modulated interface dipole within CNTs/Si interface should account for the S-shaped *I-V* characters. However, the ionic liquid gate is directly in contact with the Si surface, thus a pure CNTs/Si interface should be adopted to study the transport behaviors of photo-carriers across the CNTs/Si interface.

In this work, we investigated the transport of photo-carriers across the CNTs/Si interface by using pure CNT film directly drawn from the spinnable CNT array. By systematically decreasing (increasing) the light intensity and increasing (decreasing) the CNT coverage on Si surface, the S-shaped *I-V* characters could be reversibly eliminated and generated, and up to 121 % power conversion efficiency increment could be obtained if the generation and transportation of photo-carriers are finely matched. A phenomenological model was proposed that as the generation of photo-carriers in Si exceeded the transportation of CNTs/Si interface, the photo-carrier recombination would occur in the space charge region, which then led to the S-shaped transport characters.

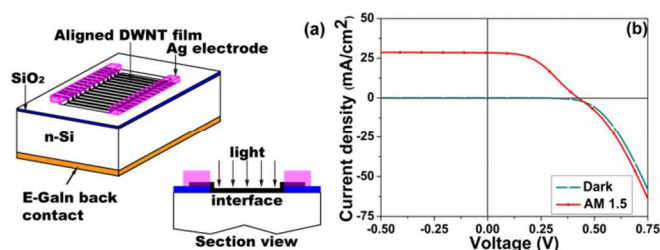


Figure 1. (a) Three-dimensional and section view of the CNTs/Si interface. (b) Typical transport *I-V* characters of CNTs/Si interface in the dark and AM 1.5G condition.

Our experiments were conducted with pure CNT film drawn from the spinnable CNT array (Fig. S1),⁶ which is more appropriate than solution processed CNT film¹⁵ due to inevitable contaminants during fabrication procedure. Fig. 1a shows the CNTs/Si interface structure with silver (Ag) and AlN electrodes, both of which have ohmic contact with CNTs and Si, respectively. The CNTs are aligned in the form of bundles, with submicron interval at distance, and aligned in the drawing direction (Fig. S2a),⁶ the film thus exhibits anisotropy

conductivity in different direction (Fig. S2b). The devices are then fabricated with 1.3 mm (parallel)×10 mm (vertical) area with the CNT film was embedded in Ag electrode, the fabrication process is described in details elsewhere.¹⁶ Thermal gravimetric (TG) analysis indicates that the CNTs are free from catalysts (Fig. S3a), and the transmission electron microscope (TEM) image shows that the CNTs are double-walled with diameter is 5 nm (Fig. S3b).

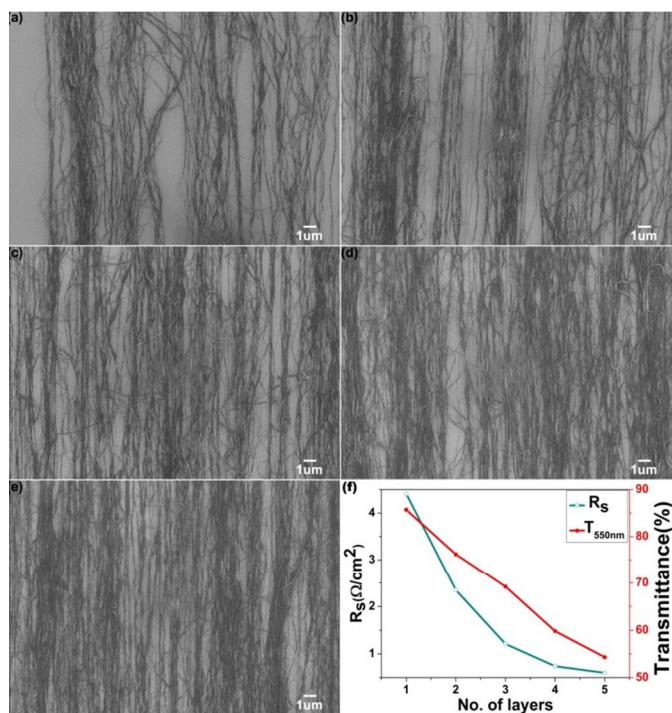


Figure 2. (a)-(e) SEM images show the effect of 1-5 layers of CNT sheet on surface coverage on a Si substrate, respectively. (f) Variation of the transmittance (at 550 nm) and R_s of the CNT film with the sheet layers

Fig. 2 (a)-(e) show the scanning electron microscope (SEM) images of 1 to 5 layers aligned CNT sheet on a Si substrate, respectively. As one layer CNT sheet was applied to the Si surface, the Si surface could not be fully covered (Fig. 2a). The coverage ratio was increased when more layers CNT sheet were applied (Fig. 2b-e). Fig. 2f reveals the transmittance was linearly decreased from 88 % to 55 % as 1-5 layers CNT sheet were applied, and the series resistance (R_s) of the CNTs/Si structure was also found to decrease but in a parabolic manner due to the overlapped CNT bundles. The decreased light transmittance and increased CNT coverage enable less generation of photo-carriers in Si and better transportation of photo-carriers across the CNTs/Si interface, respectively. The photo-carrier generation rate follows:

$$G = \alpha N_0 e^{-\alpha x} \quad (1)$$

where N_0 is the photon flux at the surface, α is the absorption coefficient, and x is the distance into the material. The equation (1) clearly shows that the generation of photo-carriers is proportional to the light intensity and the highest generation occurs at the Si surface (CNTs/Si interface).

To understand the transport of photo-carriers across the CNTs/Si interface, generation and transportation of photo-carriers have been systematically tuned by controlling the light intensity and CNT coverage on Si surface, respectively. First, the generation of photo-carriers was reduced by decreasing the light intensity from 100 mW/cm^2 to 0.6 mW/cm^2 for two layer CNTs/Si cells (Fig.3a), the second derivative curves of current to voltage (d^2I/dV^2) are

plotted in Fig. 3c to elucidate the effect of light intensity variation, and the cell parameters extracted from each curve in Fig. 3a are listed in Table 1. Fig. 3a shows a dramatic, reversible and steady evolution behavior of the transport characters with decreased light intensity. At the light intensity of 100 mW/cm^2 condition, photo-carriers transporting across the CNTs/Si interface exhibited a typical S-shaped character. As the light intensity was decreased, the S-shaped character was gradually weakened and finally eliminated at the light intensity of 0.6 mW/cm^2 condition, which is clearly indicated by a gradually disappeared peak in the d^2I/dV^2 curves (Fig. 3c). For the two layers CNTs/Si based cells, high generation of photo-carriers in Si led to the S-shaped characters while low generation not.

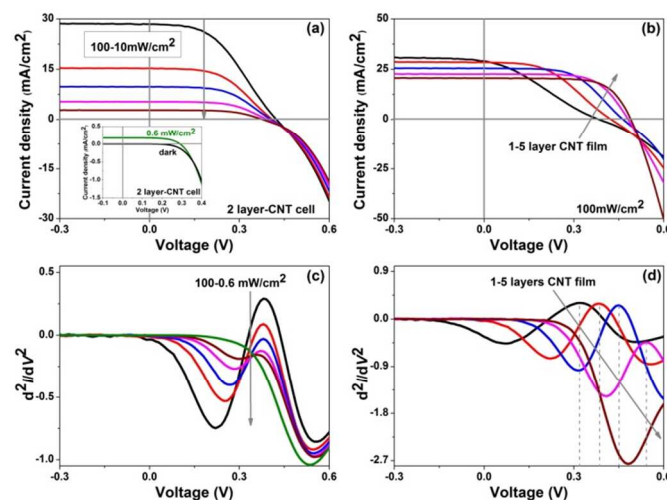


Figure 3. Evolution of the transport characters (a), and the corresponding d^2I/dV^2 curves (c) of the 2 layers CNTs/Si based cells under 100 mW/cm^2 to 0.6 mW/cm^2 condition, respectively. Evolution of the transport characters (b), and the corresponding d^2I/dV^2 curves (d) of 1-5 layers CNTs/Si based cells with fixed 100 mW/cm^2 condition.

Table 1: Parameters extracted from Fig.3a

Light (mW/cm^2)	100	52.5	33.7	18.3	9.33	0.6
V_{oc} (V)	0.42	0.41	0.41	0.39	0.38	0.29
I_{sc} (mA/cm^2)	28.3	15.3	9.8	5.26	2.77	0.17
FF	44.7	49.7	52.4	57.4	59.4	61.6
<i>PCE</i> (%)	5.31	5.94	6.25	6.40	6.70	5.68

Table 2: Parameters extracted from Fig.3b

CNT layers	1	2	3	4	5
V_{oc} (V)	0.38	0.42	0.46	0.47	0.49
I_{sc} (mA/cm^2)	29	28.4	25.4	22.6	20.5
FF	28.5	44.7	56.2	64.5	69.1
<i>PCE</i> (%)	3.14	5.34	6.56	6.70	6.94

Normally, the power conversion efficiency (*PCE*) of a crystal Si solar cell would decrease as light intensity was decrease. However,

the *PCE* of such a CNTs/Si based cell was steadily increased from 5.31 % to 6.70 % as light intensity was decreased from 100 mW/cm² to 9.33 mW/cm². However, at the light intensity of 0.6 mW/cm², the *PCE* was decreased to 5.68 %, which should be ascribed to the relative low shunt resistance.¹⁷ Table 1 shows the maximum effect contributed by the gradually eliminated S-shaped characters is the fill factor (*FF*) of cells, which was dramatically increased from 44.7 % to 61.6 %.

Fig. 3b shows the evolution of the transport characters of 1-5 layers CNTs/Si based cells under fixed light intensity of 100 mW/cm², the d^2I/dV^2 curves are plotted in Fig. 3d to elucidate the effect of CNT coverage on Si surface, and the cell parameters extracted from Fig. 3b are reported in Table 2. Fig. 3b shows that as more layers CNT sheet were applied, the transport characters of photo-carriers varied in a different manner. This can be clearly observed in Fig. 3d, where the peak, marked by dashed line, was shifted to larger voltage as more layers CNT sheet were introduced, and finally disappeared at 5 layers CNT sheet. In comparison, the peak in Fig. 3c maintained at the same voltage during light intensity variation process. Meanwhile, the open-circuit voltage (V_{oc}) of such a cell was increased from 0.38 V to 0.49 V as more layers CNT sheet were introduced (Table 2). Normally, the decreased light intensity, due to more layers CNT sheet were applied, would lead to decreased V_{oc} . However, in our system, the transmittance was decreased from 88 % to 55 %, but the V_{oc} was increased from 0.38 V to 0.49 V, which could be ascribed to the depressed photo-carrier recombination. Here, the *FF* was greatly increased from 28.5 % to 69.1 % as the S-shaped transport characters were eliminated, and then the *PCE* was increased from 3.14 % to 6.94 %, about 121 % increment. For the 100 mW/cm² illuminated condition, better CNT coverage on Si surface could completely remove the S-shaped characters.

From the above results, it can be found that for specific CNT layers sheet (two layers), the S-shaped transport characters could be eliminated when the light intensity was decreased to a threshold value (0.6 mW/cm²). Moreover, for specific light intensity (100 mW/cm²), the S-shaped transport characters could also be eliminated when the CNT layers were increased to a threshold value (5 layers). We then studied the threshold light intensity for 1 to 4 layers CNTs/Si based cells and plotted the results in Fig. 4. It can be seen that as more layers CNT sheet were applied, the threshold light intensity was also increased, exhibiting a variation manner similar to the R_s variation shown in Fig. 2f.

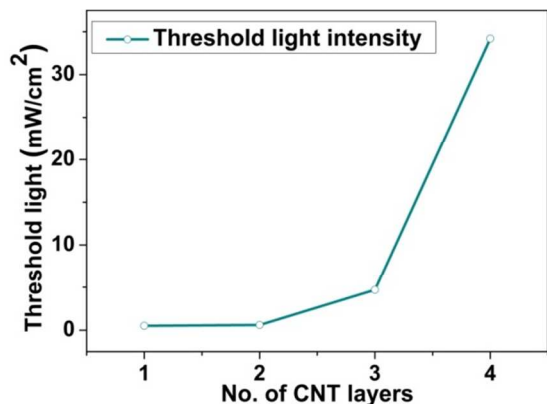


Figure 4: Threshold light intensity of 1 to 4 layers CNTs/Si, below which the S-shaped characters could be eliminated.

Generation of photo-carriers in Si and their transportation across the CNTs/Si interface is critical for high performance CNTs/Si based cells or photodetectors. The CNTs/Si interface, consisting of thousands of tiny nano junctions, sometimes is not appropriate to

balance the generation and transportation of photo-carriers, especially when single one layer CNT sheet was applied, where the CNT coverage on Si surface is poor. Actually, the S-shaped transport characters were also observed in single one layer or two layers graphene/Si based cells, when more layers graphene sheet were applied, the S-shaped transport characters could also be eliminated, and the *PCE* of the graphene/Si based cells could be increased.¹⁸

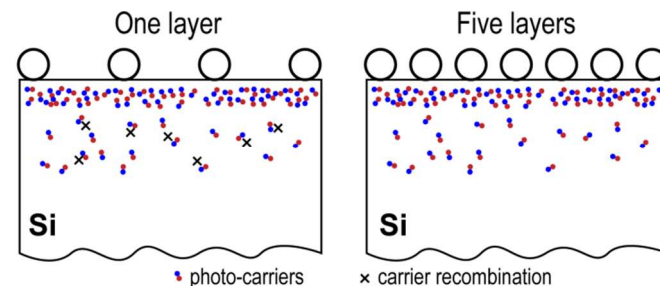


Figure 5: Schematic illustration of the separation and recombination of photo-carriers at the CNTs/Si interface formed by one and five layers CNT sheet.

The characterization of CNTs/Si based cells is usually conducted at 100 mW/cm² condition (AM 1.5G), and the largest generation of photo-carriers occurs at the Si surface (CNTs/Si interface), thus the effective transportation of photo-carriers is critical for high performance CNTs/Si based cells. To explain the observed transport characters in different layers CNTs/Si based cells, a phenomenological model was proposed (Fig. 5). At one layer CNTs/Si based cells, the CNT coverage on Si surface was poor, the transportation of photo-carriers could be hindered due to fewer transport paths, which led to carrier recombination, and then the S-shaped transport characters were generated. In comparison, as five layers CNT sheet were applied, photo-carriers generated in Si could effectively transport across the CNTs/Si interface, thus the carrier recombination was depressed and the S-shaped characters were eliminated.

Conclusions

In summary, pure CNT film drawn from the spinnable CNT array has been used to study the transport characters of photo-carriers across the CNTs/Si interface. The mismatch between the generation of photo-carriers in Si and the transportation across the CNTs/Si interface led to the S-shaped characters, the low CNT coverage on Si surface and poor conductivity of CNTs are the main sources for the limited transportation capability. The performance of CNTs/Si based solar cell was largely improved when the S-shaped transport characters were eliminated by decreasing the light intensity or increasing the CNT coverage. Our findings bring to light new design considerations for nano-junction based hybrid solar cells for energy harvest.

Acknowledgements

The work was sponsored by the National Natural Science Foundation of China (No. 21273269, 10834004), National Basic Research Program of China (No. 2011CB932600, 2012CB932402), and Knowledge Innovation Program (No. KJCX2.YW.M12) by the Chinese Academy of Sciences.

Notes and references

1. Y. Jia, A. Cao, X. Bai, Z. Li, L. Zhang, N. Guo, J. Wei, K. Wang, H. Zhu, D. Wu and P. M. Ajayan, *Nano Lett*, 2011, **11**, 1901-1905.
2. Y. Jung, X. Li, N. K. Rajan, A. D. Taylor and M. A. Reed, *Nano Lett*, 2012, **13**, 95-99.
3. E. Shi, H. Li, L. Yang, L. Zhang, Z. Li, P. Li, Y. Shang, S. Wu, X. Li, J. Wei, K. Wang, H. Zhu, D. Wu, Y. Fang and A. Cao, *Nano Lett*, 2013, **13**, 1776-1781.
4. J. Wei, Y. Jia, Q. Shu, Z. Gu, K. Wang, D. Zhuang, G. Zhang, Z. Wang, J. Luo, A. Cao and D. Wu, *Nano Letters*, 2007, **7**, 2317-2321.
5. E. Shi, L. Zhang, Z. Li, P. Li, Y. Shang, Y. Jia, J. Wei, K. Wang, H. Zhu, D. Wu, S. Zhang and A. Cao, *Sci. Rep.*, 2012, **2**.
6. J. Di, Z. Yong, X. Zheng, B. Sun and Q. Li, *Small*, 2013, **9**, 1367-1372.
7. Y. Jia, J. Wei, K. Wang, A. Cao, Q. Shu, X. Gui, Y. Zhu, D. Zhuang, G. Zhang, B. Ma, L. Wang, W. Liu, Z. Wang, J. Luo and D. Wu, *Advanced Materials*, 2008, **20**, 4594-4598.
8. Y. Jia, P. Li, X. Gui, J. Wei, K. Wang, H. Zhu, D. Wu, L. Zhang, A. Cao and Y. Xu, *Applied Physics Letters*, 2011, **98**, 133115.
9. A. Ambrosio, C. Aramo, R. Battiston, P. Castrucci, M. Cilmo, M. De Crescenzi, E. Fiandrini, V. Grossi, F. Guarino, P. Maddalena, E. Nappi, M. Passacantando, G. Pignatell, S. Santucci, M. Scarselli, A. Tinti, A. Valentini and M. Ambrosio, *Journal of Instrumentation*, 2012, **7**.
10. Y. B. An, H. Rao, G. Bosman and A. Ural, *Journal of Vacuum Science & Technology B*, 2012, **30**.
11. P. Wadhwa, B. Liu, M. A. McCarthy, Z. Wu and A. G. Rinzler, *Nano Lett*, 2010, **10**, 5001-5005.
12. P. Wadhwa, G. Seol, M. K. Petterson, J. Guo and A. G. Rinzler, *Nano Letters*, 2011, **11**, 2419-2423.
13. A. Kumar, S. Sista and Y. Yang, *J. Appl. Phys.*, 2009, **105**, -.
14. A. Wagenpfahl, D. Rauh, M. Binder, C. Deibel and V. Dyakonov, *Phys. Rev. B*, 2010, **82**.
15. P. L. Ong, W. B. Euler and I. A. Levitsky, *Nanotechnology*, 2010, **21**, 105203.
16. R. Li, J. Di, Z. Yong, B. Sun and Q. Li, *J. Mater. Chem. A*, 2014, **2**, 4140.
17. G. E. Bunea, K. E. Wilson, Y. Meydbray, M. P. Campbell and D. M. De Ceuster, Low light performance of mono-crystalline silicon solar cells, 2006.
18. X. Li, D. Xie, H. Park, T. H. Zeng, K. Wang, J. Wei, M. Zhong, D. Wu, J. Kong and H. Zhu, *Advanced Energy Materials*, 2013, **3**, 1029-1034.

^aUniversity of Chinese Academy of Science, Yuquan Road 19, Beijing, 100049, China..

^bSuzhou Institute of Nano-Tech and Nano-Bionics, Ruoshui Road 398, Suzhou, 215123, China. Email: qwli2007@sinano.ac.cn

†Electronic Supplementary Information (ESI) available: [details of any supplementary information available should be included here]. See DOI: 10.1039/c000000x/